Published in: Materials Science & Engineering: B (1998), vol. 53, iss. 1-2, pp. 198-202.
Status: Postprint (Author's version)

AC susceptibility data on Dy_2O_3 seeded randomly oriented Dy-123 mono domains melt-textured superconductor

Ph. Vanderbemden [a], H. Bougrine [a], M. Ausloos [b], F. Auguste [c], R. Cloots [c]

[a] *SUPRAS University of Liège, Montefiore Electricity Institute, B28, Sart-Tilman, B-4000 Liège, Belgium*
[b] *SUPRAS University of Liège, Physics Institute, B5, Sart-Tilman, B-4000 Liège, Belgium*
[c] *SUPRAS University of Liège, Chemistry Institute, B6, Sart-Tilman, B-4000 Liège, Belgium*

Abstract

Dy-123 superconducting ceramics have been grown using small Dy_2O_3 single-crystals as seeds. Randomly oriented large mono-domains have been observed in the vicinity of the seeding single crystal. These domains are one order of magnitude greater in volume than the seed. The AC susceptibility versus temperature curves have been measured in a polycrystalline cubic sample for different orientations of the magnetic field with respect to the sample and for amplitudes up to 20 G. Three measuring coils, each parallel to one side of the sample, were used to investigate the anisotropy of the properties. Electrical resistance versus temperature and flux profiles at 77 K were also explored. The results show good grain connectivity. A non negligible part of the magnetic shielding is due to currents flowing inside the grains.

Keywords : $DyBa_2Cu_3O_7$ superconductor ; AC susceptibility ; flux profiles ; anisotropy

1. Introduction

Bulk polycrystalline high-T_c superconductors (HT_cS) are generally composed of grains which are sometimes separated by non-stoichiometric secondary phases. This granularity has a profound effect on the critical current density which is usually reduced severely at grain boundaries. In addition to grain boundaries, microcracks are found, mostly in the *ab*-plane. All these defects restrict the transport current in the sample. Consequently, different kinds of measurements are needed in order to understand the current limitation mechanisms and magnetic flux penetration in these materials. Moreover, data should be related to the sample microstructure and discussed within this context.

This study focuses on the electric and magnetic properties of a polycrystalline $DyBa_2Cu_3O_7$ bulk superconductor synthetized using a small Dy_2O_3 single crystal as a top seed. The synthesis process has been described in detail in a previous study [1]. The microstructure of such a material consists of a few randomly oriented large single-domains in the vicinity of the single crystal seed. These domains are one order of magnitude greater in volume than the seed.

The experimental techniques are presented in Section 2. Section 3 presents the electrical resistance, AC magnetic susceptibility and flux profile data. In Section 4, the anisotropy of the out-of-phase component (χ'') of the AC susceptibility is briefly discussed and related to the microstructural observations.

2. Experimental details

Magnetic susceptibility and critical current measurements were performed in a home-made susceptometer based on a CTI-21 model cryocooler. No metallic material was present in the vicinity of the sample. The sample geometry was chosen to be a cube (side length 3 mm) with rounded edges. In this way the demagnetization factor is $\approx 1/3$ (SI) and nearly independent of the field orientation. This allows us to attribute any angular dependence of the susceptibility to the sample microstructure and not to geometric effects. The AC field was generated by a home-made electromagnet made up of a iron core sheet and four generating coils driven by an HP8904 synthetizer followed by a C-audio ST 600 power amplifier. The frequency was fixed at 1053 Hz.

Fig. 1 shows a sketch of the technical process used for the measurements. A small cube was cut from the initial ceramic pellet. The *z*-axis denotes the direction perpendicular to the largest side of the pellet. Three orthogonal 15 turn coils of fine copper wire (50 μm diameter) were wrapped tightly around the sample to form three pick-up coils sensing the sample response to the AC magnetic flux in the direction of the coil axis. The numbers 1, 2, 3 refer to the coils perpendicular to the *x, y* and *z*-axis, respectively. Since the pick-up coils were very close to the sample surface, the measured signal was assumed to be directly proportional to the magnetic flux through the specimen and no compensating coil was used. An optical polarized light picture of the sample (Fig. 1) shows the cross section parallel to the *xy*-plane. Large monodomains are clearly visible in this figure.

Published in: Materials Science & Engineering: B (1998), vol. 53, iss. 1-2, pp. 198-202.
Status: Postprint (Author's version)

Electrical resistivity versus temperature measurements were performed using a standard four-probe technique. The measuring current was reversed at each temperature in order to eliminate thermoelectric effects.

Fig. 1. *(a) Configuration of the sensing coils, β denotes the angle between the applied magnetic field and the y-direction in the xy-plane. (b) Optical polarized light micrograph of the Dy-123 melt-textured sample.*

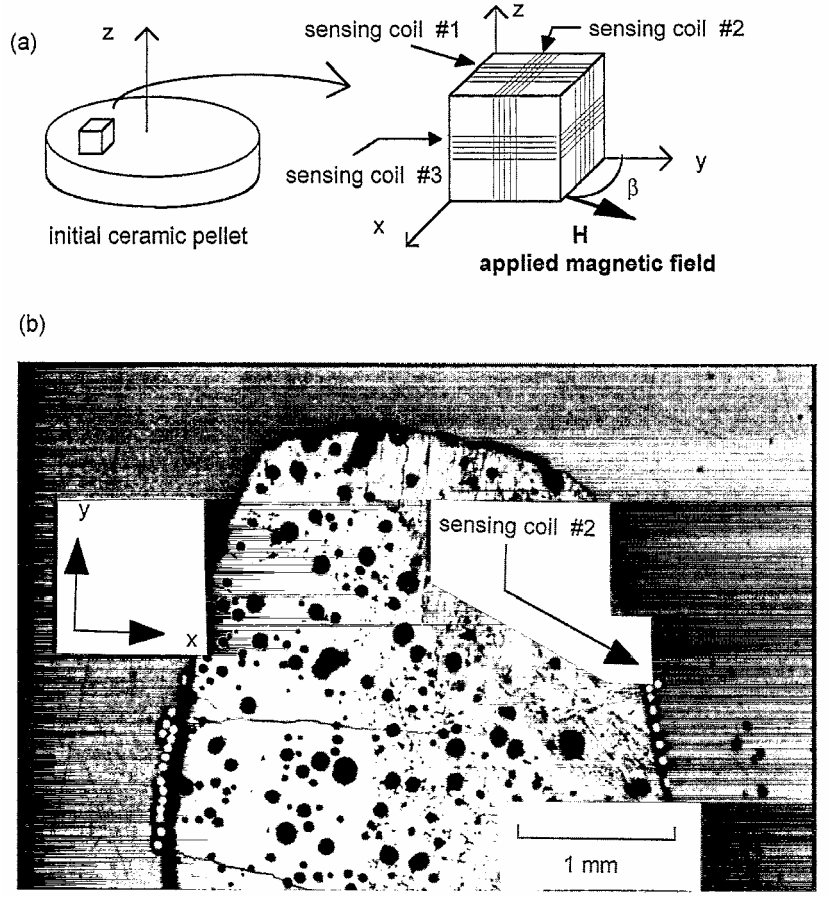

3. Results and discussion

3.1. Electrical resistivity and AC susceptibility

Fig. 2 shows the temperature dependence of the electrical resistivity (top) and AC magnetic susceptibility (bottom). Both experiments were performed in the same current geometry, i.e. $H_{AC} \parallel z$-axis for AC susceptibility measurements (inducing screening currents in the *xy*-plane) and $I \parallel xy$-plane for resistivity measurements. The voltage leads used in resistivity measurements spanned several domain boundaries.

The resistivity transition width is quite narrow (0.6 K). The $\rho(T)$ curve goes to zero at T_{C0} = 88.5 K, corresponding to the establishment of a percolative current path through the sample. Under DC applied magnetic fields up to 0.3 T, the transition region slightly broadens, but no foot is seen below the critical temperature as would be the case in ceramics containing weak links. This observation suggests that the grains present in this ceramic are strongly connected in that they can sustain a well defined intergranular current, even at 0.3 T. The critical temperature measured at the inflexion point of the $\rho(T)$ curve is 89.2 K.

The imaginary (χ'') part of AC susceptibility exhibits two peaks. The high-temperature peak represents an intragranular transition since it appears at $T > T_{C0}$. The low-temperature peak occurring at $T < T_{C0}$ characterizes a coupling between neighbouring grains. Such a double-peak structure is usually encountered in weakly coupled ceramics. In the case of the present samples, we emphasize that the temperature difference between both peaks is small (< 3 K). Hence the intergranular coupling is quite efficient. Both peaks amplitudes are comparable, a non negligible part of the magnetic shielding is then due to currents flowing inside the grains.

Fig. 2. *Electrical resistivity measured at several DC magnetic fields (top) and AC susceptibility (bottom) as a function of temperature B_{AC} = 1 G, f = 1053 Hz.*

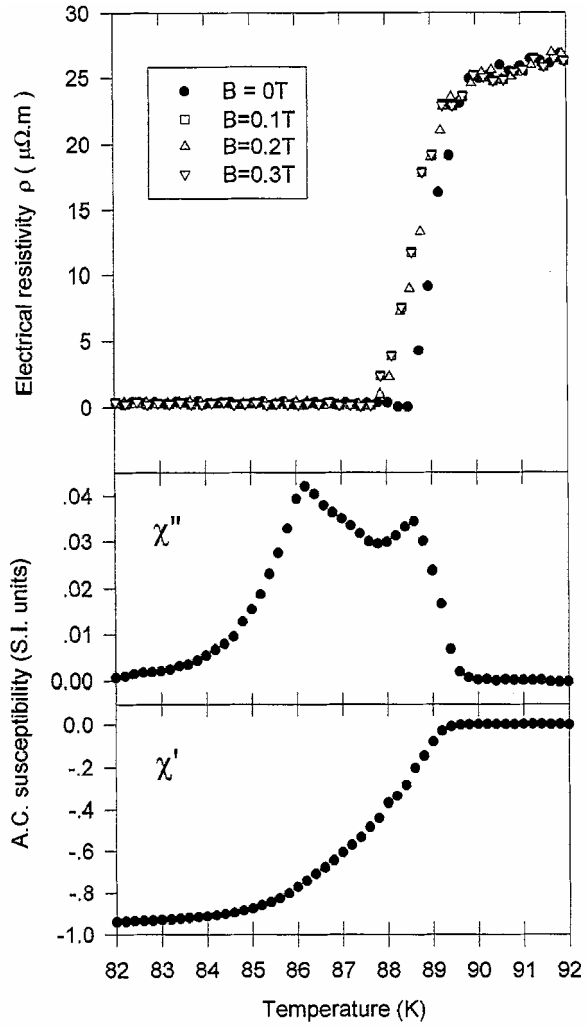

3.2. Flux profiles

Flux profiles were determined at the temperature T = *77* K and a frequency f = 1053 Hz by using the Campbell method [2]. Fig. 3 displays the results obtained (a) at zero DC magnetic field and (b) by applying different DC fields parallel to the AC field.

The plot of the AC magnetic field amplitude b against dΦ/db measured for zero DC field on granular superconductors usually shows a well marked discontinuity [3], due to the relatively low value of the intergranular current compared to the intragranular value. Such a measurement (Fig. 3(a)) carried out on the Dy-123 sample exhibits a very smooth inflexion point at $\mu_0 H_{AC} \approx 80$ G but does not show clear features pointing to either inter- or intra-grain origin, even for AC inductions as large as 300 G.

Similar observations result from the flux profiles determined by superimposing a large DC magnetic field to a small ripple AC magnetic field (Fig. 3(b)). In this case the critical current is assumed to be independent on the AC field amplitude and the variable p represents the flux lines penetration depth into the sample. Usually a shoulder is predicted when weak links are present. This shoulder generally allows to deduce both intergranular (J_{ci}) and intragranular (J_{cg}) critical current densities from the slopes of the flux profile on both sides of the shoulder [4-6]. This is not the case here, where flux profiles are rather linear.

In order to explain this behaviour let us recall that J_{cg} and J_{ci} critical current densities can be separated from flux profile data only for specimens fulfilling the condition $J_{cg}R_g > J_{ci}R$, where R and R_g denote the radius of the sample and of the grains, respectively [6]. The value and the physical significance of the parameter R_g requires careful consideration. In weakly coupled superconducting materials with a relatively small grain size (< 5 μm), R_g is usually taken as the mean grain radius. Such a situation arises for non-textured BSSCO-2223 ceramics [7].

Published in: Materials Science & Engineering: B (1998), vol. 53, iss. 1-2, pp. 198-202.
Status: Postprint (Author's version)

However, for materials with large grains, the current loops within the grains can flow in significantly smaller subregions than the grain size. This is due to the existence inside the grains of twin planes or cracks acting as effective grain boundaries [8,9]. With this interpretation in mind, R_g does not then represent the mean grain size but is rather a characteristic diameter of the current loops and is determined by the defects inside the grains. By taking into account a small R_g value in our Dy-123 sample and a high grain connectivity (Fig. 2), the condition $J_{cg}R_g > J_{cj}R$ is not fulfilled, which explains the only one slope present in the flux profiles.

Fig. 3. *Flux profiles obtained following the Campbell procedure at T = 77 K, f = 1053 Hz. p/R is the normalized magnetic flux penetration depth from the sample surface. p/R is proportional to dF/db, where F and b represent the magnetic flux through the sample and the applied induction amplitude, respectively, (a) zero DC magnetic field (b) different DC magnetic fields ($\mu_0 H_{DC}$ from 40 to 240 G).*

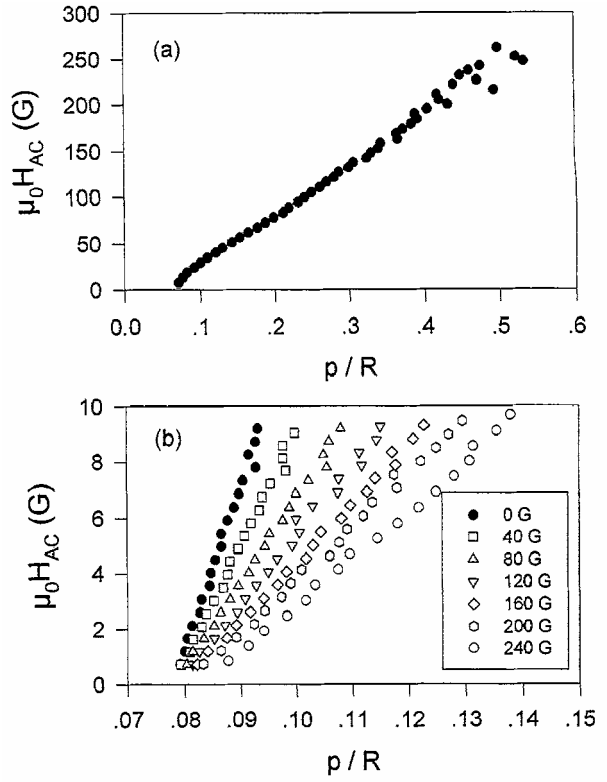

4. AC susceptibility anisotropy

Fig. 4(a) summarizes the out-of phase component (χ'') of the AC susceptibility versus temperature measured for the *x, y* and *z*-field orientations. No particular anisotropy effect can be seen.

When the magnetic field is tilted from the principal axes of the sample, magnetic flux is picked up by two or three of the sensing coils. Fig. 4(b) serves as an illustration for a 20 G applied induction making an angle β with respect to the *y* axis. The shielding currents are measured both by coil # 1 or # 2. Results show that the onset temperature is nearly independent of the β orientation but differs by 2.5 K for coils # 1 and # 2. Hence the *y* component of the magnetic field (measured by the coil # 2) is screened much better than the *x* component (measured by the coil # 1). This means that shielding currents flow more easily in the *xz*-plane that in the *yz*-plane. This observation is not in contrast with the microstructure of the largest grain of the sample (left-side of the picture presented in Fig. 1) for which *ab*-planes (parallel to the cracks) are oriented along the *x*-direction.

Fig. 4. *(a) χ" versus temperature curves measured for magnetic field parallel to x, y and z-axis, respectively, (b) χ" versus temperature curves measured either by coil # 1 and # 2 for a 20 G applied induction making an angle β with respect to the y-axis.*

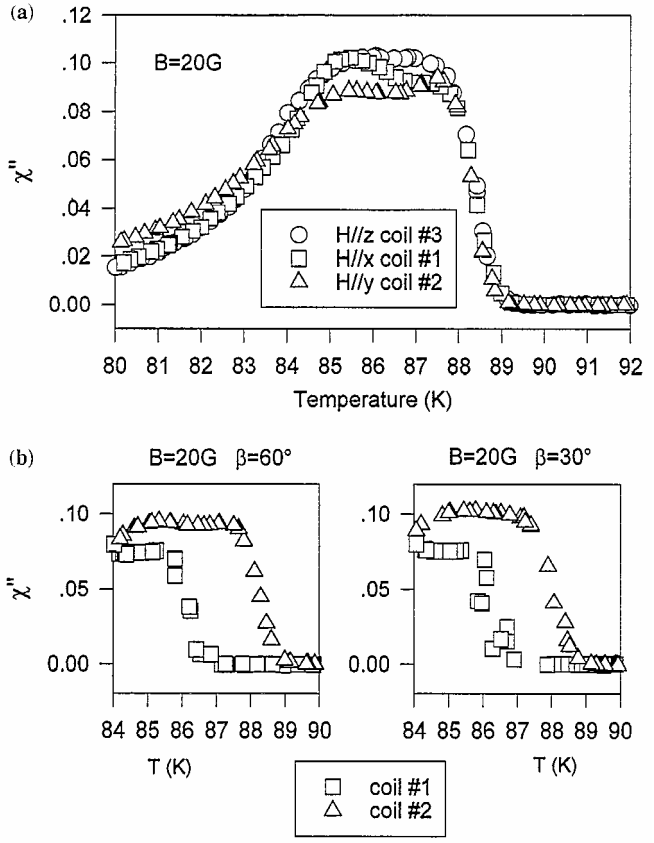

5. Conclusions

The magnetic and electric properties of a Dy-123 bulk material synthetized by using a dysprosium oxide single crystal as seed were investigated. Results show a large magnetic intragrain shielding and a good grain connectivity. Consequently this synthesis process seems to be an interesting alternative means of producing large superconducting 123 monodomains.

Acknowledgements

Ph. V. is grateful to the FNRS for a research grant. This research work is supported by an U.Lg. Action de Recherches Concertées (ARC 94-99/174) grant from the Ministery of Higher Education through the University of Liège Research Council.

References

[1] R. Cloots, F. Auguste, A. Rulmont, N. Vandewalle, M. Ausloos, J. Mater. Res. 12 (1997) 3199.

[2] A.M. Campbell, J. Phys. C 2 (1969) 1492.

[3] A.M. Campbell, F.J. Blunt, Phys. C 172 (1990) 253.

[4] R. Cloots, A. Dang, P. Vanderbemden, A. Vanderschueren, H. Bougrine, H.W. Vanderschueren, A. Rulmont, M. Ausloos, Z. Phys. B 100 (1996) 551.

[5] P.A. Godelaine, M. Ausloos, Solid State Commun. 76 (1990) 785.

[6] H. Küpfer, I. Apfelstedt, R. Flükiger, et al., Cryogenics 28 (1988) 650.

[7] P. Vanderbemden, C. Destombes, R. Cloots, M. Ausloos, presented at SMART97 conference in Liège, Belgium, June 25-27, 1997,

[8] H. Küpfer, I. Apfelstedt, R. Flükiger, C. Keller, et al., Cryogenics 29 (1989) 268.

[9] E.S. Otabe, N. Ohtani, T. Matsushita, Y. Ishikawa, S. Yoshizawa, Jpn. J. Appl. Phys. 33 (1994) 996.